Time-reversal asymmetries in Λ_b semileptonic decays

Chao-Qiang Geng,[*] Xiang-Nan Jin,[†] and Chia-Wei Liu[‡]

School of Fundamental Physics and Mathematical Sciences, Hangzhou Institute for Advanced Study, University of Chinese Academy of Sciences, Hangzhou 310024, China
and University of Chinese Academy of Sciences, 100190 Beijing, China

(Received 8 July 2022; accepted 14 September 2022; published 26 September 2022)

We study the decays of $\Lambda_b \to \Lambda_c(\to B_n f)\ell^-\bar{\nu}$ with $\ell = e, \mu, \tau$, where B_n and f are the daughter baryon and the rest of the particles in Λ_c cascade decays, respectively. In particular, we examine the full angular distributions with polarized Λ_b and lepton mass effects, in which the time-reversal asymmetries are identified. We concentrate on the decay modes of $\Lambda_b \to \Lambda_c(\to pK^-\pi^+)\ell^-\bar{\nu}$ to demonstrate their experimental feasibility. We show that the observables associated with the time-reversal asymmetries are useful to search for new physics as they vanish in the standard model. We find that they are sensitive to the right-handed current from new physics, and possible to be observed at LHCb.

DOI: 10.1103/PhysRevD.106.053006

I. INTRODUCTIONS

The transitions of $b \to c\ell^-\bar{\nu}$ with $\ell = e, \mu, \tau$ have raised great interest in both the theoretical and experimental aspects [1,2]. In particular, the discrepancy of $R_{D^{(*)}} = \Gamma(\bar{B} \to D^{(*)}\tau^-\bar{\nu})/\Gamma(\bar{B} \to D^{(*)}l^-\bar{\nu})$ with $l = e, \mu$ has shown that the possible contributions from new physics (NP) can be as large as $\mathcal{O}(10\%)$. Explicitly, we have that $R^{\rm exp}_{D,D^*} = (0.340 \pm 0.030, 0.295 \pm 0.014)$ from the experiments [2–4] and $R^{\rm SM}_{D,D^*} = (0.304 \pm 0.003, 0.259 \pm 0.006)$ from the lattice QCD calculation [5], implying that NP can play a significant role. For a review, one is referred to Ref. [6].

On the other hand, LHCb has recently announced the baryonic version of the ratio to be $R_{\Lambda_c} = \Gamma(\Lambda_b \to \Lambda_c\tau^-\bar{\nu})/\Gamma(\Lambda_b \to \Lambda_c l^-\bar{\nu}) = 0.242 \pm 0.026 \pm 0.040 \pm 0.059$ [7], where the first and second uncertainties are statistical and systematic, respectively, and the third one comes from the normalization channel of $\Lambda_b \to \Lambda_c\pi^+2\pi^-$. In contrast to $R_{D^{(*)}}$, R_{Λ_c} is found to be larger in theory, given as $R_{\Lambda_c} = 0.324 \pm 0.004$ based on lattice QCD [8]. Such opposite behavior indicates that there would be some theoretical errors, which have not been properly considered. Thus, as a complementarity, it is useful to examine the angular distributions [9–11]. In most of the works in the literature, Λ_b is assumed to be unpolarized. However, it is important to analyze the polarized cases, since the polarization fraction P_b is recently found to be around 3% in proton-proton collisions at center-of-mass energies of 13 TeV [12]. We emphasize that with $P_b \neq 0$, the time-reversal (TR) asymmetries can be observed without the cascade decays of Λ_c as we will show in this work. Moreover, the value of 3% is twice larger than $\mathcal{B}(\Lambda_c \to \Lambda\pi^+, pK^0_S)$, and hence it is useful to study the cases with $P_b \neq 0$ for probing the TR asymmetries.

The angular distribution of $\Lambda_b \to \Lambda_c(\to pK^0_S)\mu^-\bar{\nu}$ with polarized Λ_b was first given in Ref. [13]. In this work, we provide the full angular distributions of $\Lambda_b \to \Lambda_c(\to B_n f)\ell^-\bar{\nu}$, where B_n is the daughter baryon and f stands for the rest of the daughter particles. In contrast to those in the literature, we extend the study to the three-body Λ_c decays to include $\Lambda_c \to pK^-\pi^+$ and $\Lambda_c \to \Lambda l^+\nu$. In particular, $\Lambda_c \to pK^-\pi^+$ has a great advantage for the experimental detection, since all the particles in the final states are charged.

In the standard model (SM), the TR asymmetries in $\Lambda_b \to \Lambda_c(\to B_n f)\ell^-\bar{\nu}$ are zero due to the absence of the weak phase in the $\Lambda_b \to \Lambda_c$ transition. Clearly, a non-vanishing TR asymmetry indicates the existence of NP with a new CP violating phase beyond the SM.

The layout of this work is given as follows. In Sec. II, we present the angular distributions of the SM parametrized by the helicity amplitudes. In Sec. III, we discuss the effects from NP, and show that they can be absorbed by redefining the helicity amplitudes. In Sec. IV, we estimate the TR asymmetries and their feasibility to be measured at LHCb. At last, we conclude the study in Sec. V.

[*] cqgeng@ucas.ac.cn
[†] jinxiangnan21@mails.ucas.ac.cn
[‡] chiaweiliu@ucas.ac.cn

II. DECAY OBSERVABLES

In the SM, the amplitudes of $\Lambda_b \to \Lambda_c \ell^- \bar{\nu}$ are dominated by the weak interaction at tree level, given as

$$\frac{G_F}{\sqrt{2}} V_{cb} g^{\mu\nu} \bar{u}_\ell \gamma_\mu (1-\gamma_5) v \langle \Lambda_c | \bar{c} \gamma_\nu (1-\gamma_5) b | \Lambda_b \rangle, \quad (1)$$

where G_F is the Fermi constant, V_{cb} corresponds to the Cabibbo-Kobayashi-Maskawa (CKM) matrix element, and u_ℓ and v are the Dirac spinors of charged leptons and antineutrinos, respectively. In this work, we do not specify the flavors of (anti)neutrinos as they cannot be distinguished in the experiments.

We further decompose the amplitudes by expanding the Minkowski metric,

$$g^{\mu\nu} = \varepsilon_t^\mu(q) \varepsilon_t^{*\nu}(q) - \sum_{\lambda=0,\pm} \varepsilon_\lambda^\mu(q) \varepsilon_\lambda^{*\nu}(q), \quad (2)$$

where $q = (q^0, \vec{q})$ and ε are the four-momentum and polarization vector of the off-shell W boson, respectively. The subscript in ε denotes the helicity, where t indicates timelike while the others spacelike. In particular, we have that

$$\varepsilon_\pm^\mu = \frac{1}{\sqrt{2}}(0, \pm 1, i, 0)^T, \qquad \varepsilon_0^\mu = (0,0,0,-1)^T,$$
$$\varepsilon_t^\mu = (-1,0,0,0)^T, \quad (3)$$

in the center of mass frame of $\ell^- \bar{\nu}$, which would be referred to as the $\vec{q}$ frame in the following. Notice that the relative phases between ε are crucial as they interfere in the decay distributions. In this work, they are fixed by the lowering operators, given by

$$(J_x - iJ_y)\varepsilon_{1,0} = \sqrt{2}\varepsilon_{0,-1}, \quad (4)$$

where $J_{x,y}$ are the $SO(3)$ rotational generators. On the other hand, in the center of the mass frame of Λ_b with $\vec{q} = -|\vec{q}|\hat{z}$, which would be referred to as the Λ_b frame, we have

$$\varepsilon_\pm^\mu = \frac{1}{\sqrt{2}}(0, \mp 1, i, 0)^T, \qquad \varepsilon_0^\mu = \frac{1}{\sqrt{q^2}}(-|\vec{q}|, 0, 0, q^0)^T,$$
$$\varepsilon_t^\mu = \frac{-1}{\sqrt{q^2}} q^\mu, \quad (5)$$

which are useful for the latter purpose.

Plugging Eq. (2) in Eq. (1), we have

$$\frac{G_F}{\sqrt{2}} V_{cb} \left(L_t B_t - \sum_{\lambda=0,\pm} L_\lambda B_\lambda \right), \quad (6)$$

and

$$B_{\lambda_W} = \varepsilon_{\lambda_W}^{*\mu} \langle \Lambda_c | \bar{c} \gamma_\mu (1-\gamma_5) b | \Lambda_b \rangle,$$
$$L_{\lambda_W} = \varepsilon_{\lambda_W}^{\mu} \bar{u}_\ell \gamma_\mu (1-\gamma_5) v, \quad (7)$$

with $\lambda_W = t, 0$ and $\pm$. Note that B_{λ_W} and L_{λ_W} depend on the polarizations of the baryons and leptons, respectively. It is clear that in Eqs. (6) and (7), the amplitudes are decomposed as the products of Lorentz scalars, describing $\Lambda_b \to \Lambda_c W^{-*}$ (B_{λ_W}) and $W^{-*} \to \ell^- \bar{\nu}$ (L_{λ_W}). A great advantage is that B_{λ_W} and L_{λ_W} can be computed independently in the Λ_b and $\vec{q}$ frames, respectively, reducing the three-body problems to the products of two-body ones.

To proceed further, we have to consider the polarizations of the baryons and leptons. To this end, it is convenient to parametrize B_{λ_W} as

$$B_{\lambda_W} = \varepsilon_{\lambda_W}^{*\mu} \bar{u}_c \left[\left(f_1(q^2)\gamma_\mu - i f_2(q^2) \frac{\sigma_{\mu\nu}}{M_b} q^\nu + f_3(q^2) \frac{q_\mu}{M_b} \right) - \left(g_1(q^2)\gamma_\mu - i g_2(q^2) \frac{\sigma_{\mu\nu}}{M_b} q^\nu + g_3(q^2) \frac{q_\mu}{M_b} \right) \gamma_5 \right] u_b, \quad (8)$$

where $f_{1,2,3}$ and $g_{1,2,3}$ represent the form factors, M_b is the mass of Λ_b, and $\sigma_{\mu\nu} = i(\gamma_\mu\gamma_\nu - \gamma_\nu\gamma_\mu)/2$. The helicity amplitudes are calculated by

$$H_{\lambda_c,\lambda_W} = B_{\lambda_W}(\lambda_b = \lambda_c - \lambda_W, \lambda_c, \vec{p}_c = -\vec{q} = |\vec{p}_c|\hat{z}), \quad (9)$$

where $\lambda_{b(c)}$ corresponds to the angular momentum (helicity) of $\Lambda_{b(c)}$, $\vec{p}_c$ is the three-momentum of Λ_c in the Λ_b frame, and the conventions of the Dirac spinors are given in Appendix A. Plugging Eq. (5) in Eq. (8), we obtain explicitly that

$$H_{\pm\frac{1}{2}\pm 1} = \sqrt{2Q_-}\left(f_1 + \frac{M_+}{M_b} f_2 \right) \pm \sqrt{2Q_+}\left(-g_1 + \frac{M_-}{M_b} g_2 \right),$$
$$H_{\pm\frac{1}{2}0} = -\sqrt{\frac{Q_-}{q^2}}\left(M_+ f_1 + \frac{q^2}{M_b} f_2 \right) \pm \sqrt{\frac{Q_+}{q^2}}\left(M_- g_1 - \frac{q^2}{M_b} g_2 \right),$$
$$H_{\pm\frac{1}{2}t} = -\sqrt{\frac{Q_+}{q^2}}\left(M_- f_1 + \frac{q^2}{M_b} f_3 \right) \pm \sqrt{\frac{Q_-}{q^2}}\left(M_+ g_1 - \frac{q^2}{M_b} g_3 \right), \quad (10)$$

where $M_\pm = M_b \pm M_c$, M_c is the mass of Λ_c, and $Q_\pm = (M_\pm)^2 - q^2$. Note that both the form factors and amplitudes depend on q^2.

On the other hand, the antineutrinos have positive helicities, and L_{λ_W} depends only on λ_ℓ the helicity of ℓ^-. From the definitions of $h_\pm$, given by

$$h_+ = L_0\left(\lambda_e = \frac{1}{2}, \vec{p}_\ell = -\vec{p}_\nu = |\vec{p}_e|\hat{z}\right),$$
$$h_- = L_{-1}\left(\lambda_e = -\frac{1}{2}, \vec{p}_\ell = -\vec{p}_\nu = |\vec{p}_e|\hat{z}\right), \quad (11)$$

we explicitly have

$$h_- = -2\sqrt{2(q^2 - m_\ell^2)}, \quad h_+ = \sqrt{\delta_\ell}h_-, \quad \delta_\ell = \frac{m_\ell^2}{2q^2}, \quad (12)$$

with Eqs. (3) and (7) with $\vec{p}_{\ell(\nu)}$ the three-momentum of $\ell^-(\bar{\nu})$ in the $\vec{q}$ frame.

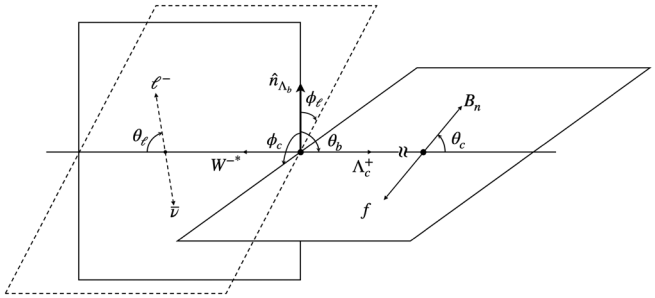

FIG. 1. Definitions of the angles, where B_n represents the daughter baryon and f the rest of the decay particles.

The angular distributions of $\Lambda_b \to \Lambda_c(\to B_n f)\ell^-\bar{\nu}$ can be obtained by piling up the Wigner-d matrices of d^J, read as

$$\frac{\partial^6\Gamma(\Lambda_b \to \Lambda_c(\to B_n f)\ell^-\bar{\nu}))}{\partial q^2 \partial\cos\theta_b \partial\cos\theta_c \partial\cos\theta_\ell \partial\phi_c \partial\phi_\ell} = \mathcal{B}(\Lambda_c \to B_n f)\frac{\zeta(q^2)}{32\pi^2}\sum_{\lambda_\ell,\lambda,\lambda_b}\rho_{\lambda_b,\lambda_b}|A_\lambda^c h_{\lambda_\ell}|^2$$
$$\times\left|\sum_{\lambda_c,\lambda_W}(-1)^{J_W}H_{\lambda_c,\lambda_W}d^{\frac{1}{2}}(\theta_b)^{\lambda_b}{}_{\lambda_c-\lambda_W}d^{\frac{1}{2}}(\theta_c)^{\lambda_c}{}_{\lambda}d^{J_W}(\theta_\ell)^{\lambda_W}{}_{\lambda_\ell-\frac{1}{2}}e^{i(\lambda_c\phi_c+\lambda_\ell\phi_\ell)}\right|^2,$$
$$\zeta(q^2) = \frac{G_F^2}{24\pi^3}|V_{cb}|^2\frac{(q^2-M_\ell^2)^2|\vec{p}_c|}{8M_b^2 q^2}, \quad (13)$$

where $\mathcal{B}(\Lambda_c \to B_n f)$ are the branching fractions of $\Lambda_c \to B_n f$, $\rho_{\pm,\pm} = (1 \pm P_b)/2$, $\lambda_{(b,c,\ell)} = \pm 1/2$, $|\vec{p}_c| = \sqrt{Q_+Q_-}/2M_{\mathbf{B}_b}$, the factor of $(-1)^{J_W}$ comes from Eq. (6) along with $J_W = 0(1)$ for $\lambda_W = t(\pm, 0)$, and A_λ^c are associated with the up-down asymmetries of $\Lambda_c \to B_n f$. Here, the definitions of the angles can be found in Fig. 1, where $\theta_{b,c}$ and θ_ℓ are defined in the center of mass frames of $\Lambda_{b,c}$ and $\ell^-\bar{\nu}$, respectively, while $\phi_{c,\ell}$ are the azimuthal angles between the decay planes.

The derivation of Eq. (13) is sketched in Appendix B. The index λ corresponds to $\lambda_{B_n} - \lambda_f$ with λ_{B_n} and λ_f the helicities of B_n and f in $\Lambda_c \to B_n f$, respectively. If f contains more than two particles, we simply group them together, forming an angular momentum eigenstate in the center-of-mass frame of f, acquiring an effective helicity.

In the case of $\Lambda_c \to pK^-\pi^+(\Lambda l^+\nu)$, A_λ^c depends on the three-momentum of $p(\Lambda)$ and angles in $K^-\pi^+$ $(l^+\nu)$ as well. However, we integrate out the dependence for simplicity in this work. In addition, the cascade decays of τ^- can be included by continually piling up the Wiger-d matrices inside Eq. (13). The interested readers are referred to Ref. [11]. Note that the overall q^2 dependence in Eq. (13) can be cast in a more symmetric form by recognizing $|\vec{p}_\ell| = (q^2 - m_\ell^2)/\sqrt{4q^2}$ in the $\vec{q}$ frame.

We expand the angular distributions as

$$\frac{\partial^6\Gamma(\Lambda_b \to \Lambda_c(\to B_n f)\ell^-\bar{\nu})}{\partial q^2 \partial\vec{\Omega}} = \mathcal{B}(\Lambda_c \to B_n f)\frac{\zeta(q^2)}{32\pi^2}\sum_{i=1}^{26}\mathrm{Re}(\mathcal{X}_i(a_\pm, b_\pm, t_\pm)\mathcal{D}_i(\vec{\Omega}))\mathcal{P}_i(\alpha, P_b), \quad (14)$$

where α are the up-down asymmetries of $\Lambda_c \to B_n f$, $\vec{\Omega} = (\theta_{b,c,\ell}, \phi_{c,\ell})$, and explicit forms of $\mathcal{X}_i$, $\mathcal{P}_i$ and $\mathcal{D}_i$ can be found in Table I, where we have taken the abbreviations,

$$a_\pm = H_{\pm\frac{1}{2},0}, \qquad b_\pm = H_{\mp\frac{1}{2},\mp 1}, \qquad t_\pm = H_{\pm\frac{1}{2},t}, \qquad |\xi^2| = |\xi_+^2| + |\xi_-^2|, \qquad |\xi_\Delta^2| = |\xi_+^2| - |\xi_-^2|, \quad (15)$$

with $\xi = a, b, t$ and $P_2 = (3\cos^2\theta_\ell - 1)/2$. The real-valued function in Eq. (14) guarantees that the partial decay widths are real. For an illustration, we have

TABLE I. The angular distributions of $\Lambda_b \to \Lambda_c(\to B_n f)\ell^-\bar{\nu}$ with $P_2 = (3\cos^2\theta_\ell - 1)/2$ and the parameters of a, b and t defined in Eq. (15).

i	$\mathcal{X}_i$	P_i	$\mathcal{D}_i$
1	$(\delta_\ell+1)(\lvert a\rvert^2+\lvert b\rvert^2)+3\delta_\ell\lvert t\rvert^2$	1	1
2	$(2\delta_\ell-1)(\lvert a\rvert^2-\frac{1}{2}\lvert b\rvert^2)$	1	P_2
3	$-6\delta_\ell(\mathrm{Re}(a_+t_+^*)+\mathrm{Re}(a_-t_-^*))+\frac{3}{2}\lvert b_\Delta\rvert^2$	1	$\cos\theta_\ell$
4	$(\delta_\ell+1)(\lvert a_\Delta\rvert^2+\lvert b_\Delta\rvert^2)+3\delta_\ell\lvert t_\Delta\rvert^2$	P_b	$\cos\theta_b$
5	$(2\delta_\ell-1)(\lvert a_\Delta\rvert^2-\frac{1}{2}\lvert b_\Delta\rvert^2)$	P_b	$\cos\theta_b P_2$
6	$-6\delta_\ell[\mathrm{Re}(a_+t_+^*)-\mathrm{Re}(a_-t_-^*)]-\frac{3}{2}\lvert b_\Delta\rvert^2$	P_b	$\cos\theta_b\cos\theta_\ell$
7	$\frac{3}{\sqrt{2}}[2\delta_\ell(t_-b_+^*-b_-t_+^*)+(a_-b_+^*+b_-a_+^*)]$	P_b	$e^{i\phi_\ell}\sin\theta_b\sin\theta_\ell$
8	$\frac{3}{\sqrt{2}}(2\delta_\ell-1)(b_-a_+^*-a_-b_+^*)$	P_b	$e^{i\phi_\ell}\sin\theta_b\sin\theta_\ell\cos\theta_\ell$
9	$(\delta_\ell+1)(\lvert a_\Delta\rvert^2-\lvert b_\Delta\rvert^2)+3\delta_\ell\lvert t_\Delta\rvert^2$	α	$\cos\theta_c$
10	$(2\delta_\ell-1)(\lvert a_\Delta\rvert^2+\frac{1}{2}\lvert b_\Delta\rvert^2)$	α	$\cos\theta_c P_2$
11	$6\delta_\ell(\mathrm{Re}(a_-t_-^*)-\mathrm{Re}(a_+t_+^*))-\frac{3}{2}\lvert b\rvert^2$	α	$\cos\theta_c\cos\theta_\ell$
12	$\frac{3}{\sqrt{2}}[2\delta_\ell(b_-t_-^*-t_+b_+^*)-(a_+b_+^*+b_-a_-^*)]$	α	$e^{i\Phi}\sin\theta_c\cos\theta_c$
13	$\frac{3}{\sqrt{2}}[2\delta_\ell(a_+b_+^*-b_-a_-^*)+(b_-a_-^*-a_+b_+^*)]$	α	$e^{i\Phi}\sin\theta_c\cos\theta_c\cos\theta_\ell$
14	$(2\delta_\ell+1)a_+a_-^*$	$P_b\alpha$	$\sin\theta_b\sin\theta_c P_2$
15	$2\delta_\ell(\lvert a\rvert^2+\lvert b\rvert^2)-(\lvert a\rvert^2+1/2\lvert b\rvert^2)$	$P_b\alpha$	$\cos\theta_b\cos\theta_c P_2$
16	$\delta_\ell(\lvert a\rvert^2-\lvert b\rvert^2+3\lvert t\rvert^2)+(\lvert a\rvert^2-\lvert b\rvert^2)$	$P_b\alpha$	$\cos\theta_b\cos\theta_c$
17	$-6\delta_\ell(\mathrm{Re}(a_+t_+^*)+\mathrm{Re}(a_-t_-^*))-\frac{3}{2}\lvert b_\Delta\rvert^2$	$P_b\alpha$	$\cos\theta_b\cos\theta_c\cos\theta_\ell$
18	$(2-4\delta_\ell)a_-a_+^*$	$P_b\alpha$	$e^{-i\phi_c}\sin\theta_b\sin\theta_c P_2$
19	$(1-2\delta_\ell)b_-b_+^*$	$P_b\alpha$	$e^{i(\phi_c+2\phi_\ell)}\sin\theta_b\sin\theta_c P_2$
20	$-2\delta_\ell(a_+a_-^*+3t_+t_-^*)-2a_+a_-^*$	$P_b\alpha$	$e^{i\phi_c}\sin\theta_b\sin\theta_c$
21	$(2\delta_\ell-1)b_-b_+^*$	$P_b\alpha$	$e^{i(\phi_c+2\phi_\ell)}\sin\theta_b\sin\theta_c$
22	$6\delta_\ell(a_+t_-^*+t_+a_-^*)$	$P_b\alpha$	$e^{i\phi_c}\sin\theta_b\sin\theta_c\cos\theta_\ell$
23	$\frac{3}{\sqrt{2}}[(b_-a_+^*-a_-b_+^*)-2\delta_\ell(b_-t_+^*+t_-b_+^*)]$	$P_b\alpha$	$e^{i\phi_\ell}\sin\theta_b\sin\theta_\ell\cos\theta_c$
24	$\frac{3}{\sqrt{2}}[(b_-a_-^*-a_+b_+^*)-2\delta_\ell(b_-t_-^*+t_+b_+^*)]$	$P_b\alpha$	$e^{i\Phi}\sin\theta_c\sin\theta_\ell\cos\theta_b$
25	$\frac{3}{\sqrt{2}}[2\delta_\ell(a_-b_+^*+b_-a_+^*)-(a_-b_+^*+b_-a_+^*)]$	$P_b\alpha$	$e^{i\phi_\ell}\sin\theta_b\sin\theta_\ell\cos\theta_c\cos\theta_\ell$
26	$\frac{3}{\sqrt{2}}[2\delta_\ell(b_-a_-^*-a_+b_+^*)-(a_+b_+^*+b_-a_-^*)]$	$P_b\alpha$	$e^{i\Phi}\sin\theta_c\sin\theta_\ell\cos\theta_b\cos\theta_\ell$

$$\mathrm{Re}(\mathcal{X}_7\mathcal{D}_7) = \frac{3}{\sqrt{2}}[\mathrm{Re}(2\delta_\ell(t_-b_+^*-b_-t_+^*)+(a_-b_+^*+b_-a_+^*))\cos\phi_\ell\sin\theta_b\sin\theta_\ell - \times\mathrm{Im}(2\delta_\ell(t_-b_+^*-b_-t_+^*)+(a_-b_+^*+b_-a_+^*))\sin\phi_\ell\sin\theta_b\sin\theta_\ell], \quad (16)$$

$$\mathrm{Re}(\mathcal{X}_{12}\mathcal{D}_{12}) = \frac{3}{\sqrt{2}}[\mathrm{Re}(2\delta_\ell(b_-t_-^*-t_+b_+^*)-(a_+b_+^*+b_-a_-^*))\cos(\phi_\ell+\phi_c)\sin\theta_c\cos\theta_c - \mathrm{Im}(2\delta_\ell(b_-t_-^*-t_+b_+^*)-(a_+b_+^*+b_-a_-^*))\sin(\phi_\ell+\phi_c)\sin\theta_c\cos\theta_c], \quad (17)$$

by the identity of $\mathrm{Re}(\mathcal{X}_i\mathcal{D}_i) = \mathrm{Re}(\mathcal{X}_i)\mathrm{Re}(\mathcal{D}_i) - \mathrm{Im}(\mathcal{X}_i)\mathrm{Im}(\mathcal{D}_i)$. For those $\mathcal{D}_i$, which are independent of $\phi_{c,\ell}$, we simply have $\mathrm{Re}(\mathcal{X}_i\mathcal{D}_i) = \mathcal{X}_i\mathcal{D}_i$. Notice that $\xi_\pm$ are real in the SM, and any observations of nonzero $\mathrm{Im}(\mathcal{X}_i)$ would be a smoking gun of NP. The angular distributions of $\overline{\Lambda_b} \to \overline{\Lambda_c}(\to \overline{B_n}\,\overline{f})\ell^+\nu$ can be obtained directly by taking $\theta_\ell \to \pi - \theta_\ell$ and $\alpha \to -\alpha$. In practice, δ_l can be taken as zero as an excellent approximation in the SM, with which $t_\pm$ can be neglected as well since they are always followed by δ_ℓ.

It is interesting to point out that, under the parity transformation, the helicity amplitudes behave differently as

$$a_\pm \to a_\mp, \qquad b_\pm \to b_\mp, \qquad t_\pm \to -t_\mp, \tag{18}$$

so that $\mathrm{Re}(\mathcal{X}_{7,12})$ and $\mathrm{Im}(\mathcal{X}_{7,12})$ are parity even and odd, respectively. If Λ_b is unpolarized ($P_b = 0$), it is clear that ϕ_c and ϕ_ℓ cannot be measured separately. In this case, it is convenient to introduce a new set of azimuthal coordinates as

$$\begin{aligned} \Phi &= \phi_\ell + \phi_c, & 0 < \Phi < 2\pi, \\ \Phi_\Delta &= \frac{1}{2}(\phi_\ell - \phi_c), & -\pi < \Phi_\Delta < \pi. \end{aligned} \tag{19}$$

To obtain the unpolarized angular distributions from the polarized ones, one can integrate over Φ_Δ and $\cos\theta_b$, in which $\mathcal{D}_{4-8,14-26}$ are zero. As a cross-check, we find that the results are identical to those given in Ref. [10].

With Table I, one can construct several observables in a model independent way. The simplest ones would be the partial and total decay widths, read as

$$\frac{d\Gamma(\Lambda_b \to \Lambda_c \ell^- \bar{\nu})}{dq^2} = \zeta(q^2)\mathcal{X}_1, \tag{20}$$

and

$$\Gamma = \Gamma(\Lambda_b \to \Lambda_c \ell^- \bar{\nu}) = \int_{m_\ell^2}^{(M_b - M_c)^2} \zeta(q^2)\mathcal{X}_1 dq^2, \tag{21}$$

respectively. It shall be clear that Γ is independent of $\Lambda_c \to B_n f$. Likewise, there are several observables that can be defined independent of $\Lambda_c \to B_n f$, and it is reasonable to measure them separately as they do not suffer from the smallness of $\mathcal{B}(\Lambda_c \to B_n f)$. In fact, the angular distributions without cascade decays can be obtained straightforwardly by integrating over $(\cos\theta_c, \phi_c)$, resulting in

$$\begin{aligned} &\frac{\partial^4\Gamma(\Lambda_b \to \Lambda_c \ell^- \bar{\nu})}{\partial q^2 \partial\cos\theta_b \cos\theta_\ell \partial\phi_\ell} \\ &= \frac{\zeta(q^2)}{8\pi}\sum_{i=1}^{8} \mathrm{Re}(\mathcal{X}_i(a_\pm, b_\pm, t_\pm)\mathcal{D}_i(\vec{\Omega}))\mathcal{P}_i(0, P_b), \end{aligned} \tag{22}$$

which is clearly independent of α. As a cross-check, we find that Eq. (22) reduces to the ones given by Ref. [14] with an appropriate substitution.

There are some quantities that deserve a closer look. The forward-backward asymmetries for $W^{-*} \to l^- \bar{\nu}$ and $\Lambda_c \to B_n f$ are defined as

$$\begin{aligned} A_{FB} &= 2\left(\int_0^1 - \int_{-1}^0\right)\Gamma_{\cos\theta_\ell} d\cos\theta_\ell \\ &= \frac{1}{\Gamma}\int_{m_\ell^2}^{(M_b - M_c)^2} \zeta(q^2)\mathcal{X}_3 dq^2, \\ A_{PL} &= \frac{2}{\alpha}\left(\int_0^1 - \int_{-1}^0\right)\Gamma_{\cos\theta_c} d\cos\theta_c \\ &= \frac{1}{\Gamma}\int_{m_\ell^2}^{(M_b - M_c)^2} \zeta(q^2)\mathcal{X}_9 dq^2, \end{aligned} \tag{23}$$

where we have adopted the shorthand notation,

$$\Gamma_{\vec{\Omega}} = \frac{1}{\mathcal{B}(\Lambda_c \to B_n f)}\frac{1}{\Gamma}\frac{\partial\Gamma(\Lambda_b \to \Lambda_c(\to B_n f)\ell^-\bar{\nu})}{\partial\vec{\Omega}}. \tag{24}$$

The up-down asymmetries A_{UD}, on the other hand, are given by

$$\begin{aligned} A_{UD} &= \frac{2}{P_b}\left(\int_0^1 - \int_{-1}^0\right)\Gamma_{\cos\theta_b} d\cos\theta_b \\ &= \frac{1}{\Gamma}\int_{m_\ell^2}^{(M_b - M_c)^2} \zeta(q^2)\mathcal{X}_4 dq^2, \end{aligned} \tag{25}$$

which require $P_b \neq 0$ for an experimental measurement.

Here, it is an appropriate place to revisit A_λ^c in Eq. (13) explicitly. We have

$$|A^c_{\pm\frac{1}{2}}|^2 = \frac{1}{2}(1 \pm \alpha), \tag{26}$$

where α are the up-down asymmetries of $\Lambda_c \to B_n f$, with the experimental values given by [3]

$$\begin{aligned} &\alpha(\Lambda_c \to \Lambda\pi^+, \Sigma^0\pi^+, \Sigma^+\pi^0, pK_s^0) \\ &= (-0.84 \pm 0.09, -0.55 \pm 0.11, -0.73 \pm 0.18, 0.2 \pm 0.5). \end{aligned} \tag{27}$$

Similarly, for the three-body Λ_c decays, we have $\alpha = A^c_{UD}$, where A^c_{UD} are defined by substituting $\Lambda_c \to B_n f$ for $\Lambda_b \to \Lambda_c \ell^- \bar{\nu}$ in Eq. (25). In particular, α are found to be

$$\alpha(\Lambda_c \to pK^-\pi^+, \Lambda l^+\nu) = (0.89 \pm 0.10, -0.32), \tag{28}$$

from the $SU(3)_F$ analysis [15] and light-front quark model [16], respectively.

The azimuthal angles are closely related to the triple product asymmetries, which flip signs under TR transformation [17]. To probe them, we define

$$\mathcal{T}_\ell = \frac{1}{P_b}\left(\int_0^\pi - \int_{2\pi}^\pi\right)\Gamma_{\phi_\ell} d\phi_\ell = -\frac{\pi^2}{8\Gamma}\int_{m_\ell^2}^{(M_b-M_c)^2} \zeta(q^2)\mathrm{Im}(\mathcal{X}_7)dq^2,$$
$$\mathcal{T}_c = \frac{1}{\alpha}\left[\left(\int_0^\pi - \int_{2\pi}^\pi\right)d\Phi\right]\left[\left(\int_0^1 - \int_{-1}^0\right)d\cos\theta_c\right]\Gamma_{\phi_\ell,\cos\theta_c}$$
$$= -\frac{2}{3\pi\Gamma}\int_{m_\ell^2}^{(M_b-M_c)^2} \zeta(q^2)\mathrm{Im}(\mathcal{X}_{12})dq^2, \tag{29}$$

which are proportional to the complex phases of $\xi_\pm$, and vanish without NP. Comparing to the direct CP asymmetries, TR asymmetries do not require strong phases, which are great advantages to probe CP violation as strong phases are absent in the semileptonic decays. Note that one can also construct other TR asymmetries from $\mathcal{X}_{8,13,18-26}$.

III. CONTRIBUTIONS FROM POSSIBLE NEW PHYSICS

Let us consider the dimension-six effective Hamiltonian from NP with left-handed neutrinos, read as

$$\mathcal{H}_{\rm eff}^N = \frac{G_F}{\sqrt{2}}V_{cb}[\bar{c}(C_S + C_P\gamma_5)b(\bar{u}_\ell P_L v) + \bar{c}\gamma^\mu(C_L P_L + C_R P_R)b(\bar{u}_\ell\gamma_\mu P_L v) + C_T(\bar{u}_\ell\sigma_{\mu\nu}P_L v)\bar{c}\sigma^{\mu\nu}b], \tag{30}$$

where $P_{R,L} = (1 \pm \gamma_5)$, $C_{S,P,R,L,T}$ are the Wilson coefficients, which are complex and depend on the lepton flavors in general, and N in the superscript indicates that NP is considered. The effects of $C_{S,P,R,L}$ can be absorbed by redefining the amplitudes as

$$a_\pm^N = (1+C_L)a_\pm + C_R a_\mp, \quad b_\pm^N = (1+C_L)b_\pm + C_R b_\mp,$$
$$t_\pm^N = (1+C_L)t_\pm + C_R t_\mp - \frac{\sqrt{Q_+ q^2}}{m_\ell}C_S f_s \pm \frac{\sqrt{Q_- q^2}}{m_\ell}C_P g_p, \tag{31}$$

where f_s and g_p are defined by

$$\langle\Lambda_c|\bar{c}(1+\gamma_5)b|\Lambda_b\rangle = \bar{u}_c(f_s + g_p\gamma_5)u_b. \tag{32}$$

The derivations can be found in Appendix B. Note that in Eq. (31), $\xi_\pm$ are calculated within the SM given in Eq. (10). The angular distributions can be easily obtained by substituting $\xi_\pm^N$ for $\xi_\pm$ in Table I. In the case of $C_{R,S,P} = 0$, the effect of C_L can be absorbed by redefining V_{cb} as $V_{cb}(1 + C_L)$, leaving the angular distributions unaltered. Therefore, in the following, we would simply take $C_L = 0$.

Let us first consider the case that $C_R \neq 0$ with $C_{S,P} = 0$. For the total decay widths, C_R would be polluted by the uncertainties of the form factors. However, we can utilize that $\xi_\pm$ are real, whereas C_R can be complex in general. Plugging Eq. (31) in Eq. (16), we arrive at

$$\mathrm{Im}(\mathcal{X}_7^N) = 3\sqrt{2}\mathrm{Im}(C_R)(a_+ b_+ - a_- b_-),$$
$$\mathrm{Im}(\mathcal{X}_{12}^N) = 3\sqrt{2}\mathrm{Im}(C_R)(a_+ b_- - a_- b_+), \tag{33}$$

where we have taken $\xi_\pm$ as real, calculated by Eq. (10).

On the other hand, the effects of $C_{S,P}$ are largely enhanced by the smallness of the lepton quark masses when $q^2/m_\ell^2 \gg 1$. Therefore, measuring $t_\pm$ in high q^2 regions would be useful to constrain the values of $C_{S,P}$. To diminish the uncertainties from the form factors, one can examine the complex phases, given by

$$\mathrm{Im}(\mathcal{X}_7^N) = \frac{3}{\sqrt{2}}m_\ell\left[-\mathrm{Im}(C_S)\sqrt{\frac{Q_+}{q^2}}f_s(b_+ + b_-) + \mathrm{Im}(C_P)\sqrt{\frac{Q_-}{q^2}}g_p(b_- - b_+)\right],$$
$$\mathrm{Im}(\mathcal{X}_{12}^N) = \frac{3}{\sqrt{2}}m_\ell\left[\mathrm{Im}(C_S)\sqrt{\frac{Q_+}{q^2}}f_s(b_+ + b_-) + \mathrm{Im}(C_P)\sqrt{\frac{Q_-}{q^2}}g_p(b_- - b_+)\right], \tag{34}$$

where we have taken $C_R = 0$. By collecting Eqs. (33) and (34), the net effects of NP on $\mathcal{T}_{\ell,c}$ are summarized as follows:

$$\mathcal{T}_\ell = -\frac{3\pi^2}{8\sqrt{2}}(\mathrm{Im}(C_R)\mathcal{Y}_R - \mathrm{Im}(C_S)\mathcal{Y}_S + \mathrm{Im}(C_P)\mathcal{Y}_P)$$
$$\mathcal{T}_c = -\frac{\sqrt{2}}{\pi}(\mathrm{Im}(C_R)\mathcal{Y}_R' + \mathrm{Im}(C_S)\mathcal{Y}_S + \mathrm{Im}(C_P)\mathcal{Y}_P), \tag{35}$$

where

$$\mathcal{Y}_R^{(\prime)} = \frac{1}{\Gamma}\int_{m_\ell^2}^{(M_b-M_c)^2} 2\zeta(a_+ b_{+(-)} - a_- b_{-(+)})dq^2,$$
$$\mathcal{Y}_S = \frac{1}{\Gamma}\int_{m_\ell^2}^{(M_b-M_c)^2} \zeta m_\ell \sqrt{\frac{Q_+}{q^2}} f_s (b_+ + b_-)dq^2,$$
$$\mathcal{Y}_P = \frac{1}{\Gamma}\int_{m_\ell^2}^{(M_b-M_c)^2} \zeta m_\ell \sqrt{\frac{Q_+}{q^2}} g_p (b_- - b_+)dq^2. \tag{36}$$

Notice that Γ also depends on $C_{R,S,P}$. However, in this work, we take $C_{R,S,P}$ as zero in Γ as a first order approximation, and therefore $\mathcal{Y}_{R,S,P}^{(\prime)}$ can be computed once the form factors are given.

To examine TR asymmetries in the experiments, we define

$$\begin{aligned}\Delta N_\ell &\equiv N(\pi > \phi_\ell > 0) - N(2\pi > \phi_\ell > \pi) = \epsilon N_{\Lambda_b} \mathcal{T}_\ell \mathcal{B}(\Lambda_b \to \Lambda_c^+ \ell^- \nu) P_b,\\ \Delta N_f &\equiv N(\pi > \phi_c > 0, \cos\theta_c > 0) + N(2\pi > \phi_c > \pi, \cos\theta_c < 0)\\ &\quad - N(\pi > \phi_c > 0, \cos\theta_c < 0) - N(2\pi > \phi_c > \pi, \cos\theta_c > 0)\\ &= \epsilon N_{\Lambda_b} \mathcal{T}_c \mathcal{B}(\Lambda_b \to \Lambda_c^+ \ell^- \nu)\mathcal{B}(\Lambda_c \to B_n f)\alpha(\Lambda_c \to B_n f),\end{aligned} \tag{37}$$

which hold at $N \to \infty$ with N the number of the observed events, where N_{Λ_b} is the numbers of Λ_b in experiments, and ϵ is the efficiency for the experimental reconstruction. To reduce the statistical uncertainties in ΔN_f, we can sum over the decay modes of Λ_c^+, given as

$$\Delta N_c = \sum_f |N_f| = \epsilon N_{\Lambda_b} \mathcal{T}_c \mathcal{B}(\Lambda_b \to \Lambda_c^+ \ell^- \nu) \sum_{B_n f} |\mathcal{B}(\Lambda_c \to B_n f)\alpha(\Lambda_c \to B_n f)|. \tag{38}$$

As $\Delta N_{\ell,c}$ are proportional to $\mathcal{T}_{\ell,c}$, a nonzero value of ΔN_ℓ or ΔN_c would be a smoking gun of NP.

The full angular distributions including the tensor operator are given in Appendix C. For simplicity, we take $C_T = 0$ in the numerical analysis, as they cannot be reduced to the form of Eq. (6), which breaks the angular analysis. In addition, the tensor operator is closely related to the scalar ones by the Fierz transformation in the leptoquark effective field theory [18].

IV. NUMERICAL RESULTS

As mentioned in Sec. III, nonzero signals of $\mathcal{T}_{\ell,c}$ can be clear evidence of CP violation from NP with $t_\pm^N$ largely enhanced in high q^2 regions by $C_{S,P}$. In Eq. (35), $\mathrm{Im}(C_{R,S,P})$ are in general free parameters of NP, whereas $\mathcal{Y}_{R,S,P}^{(\prime)}$ can be computed by the form factors. In this work, we utilize the homogeneous bag model to estimate the form factors [19], which agree well with those by the lattice QCD calculation as well as the heavy quark symmetry [8].

The values of $\mathcal{Y}_{R,S,P}^{(\prime)}$ are listed in Table II, from which one can see that $\mathcal{Y}_R$ and $\mathcal{Y}_R'$ are both sizable for all flavors, giving us a good opportunity to examine $\mathrm{Im}(C_R)$. In contrast, the values of $\mathcal{Y}_{S,P}$ for $\ell = e$ and μ are suppressed due to m_ℓ. For $\ell = \tau$, $\mathcal{Y}_{S,P}$ are still 3 times smaller than $\mathcal{Y}_R^{(\prime)}$. Hence, $\mathrm{Im}(C_{S,P})$ are much more difficult to be observed in the experiments comparing to $\mathrm{Im}(C_R)$.

To explain the excesses of $R_{D^{(*)}}$, $C_{R,S,P}$ are found to be tiny for $\ell = e$ and μ, but fortunately, $C_R = \pm 0.42(7)i$ is huge for $\ell = \tau$ [18]. We have plotted $\zeta(\partial\mathcal{Y}_R^{(\prime)}/\partial q^2)$ for $\ell = \tau$ in Fig. 2, where the bands represent the uncertainties from the form factors. One can see that the ideal q^2 region to search for the asymmetries lies around 7 $\mathrm{GeV}^2 < q^2 <$ 9 GeV^2, since they are huge within the region. Finally, putting the values of $\mathcal{Y}_R^{(\prime)}$ and $C_R = \pm 0.42(7)i$ in Eq. (35), we find that

$$\mathcal{T}_\ell = \pm 0.16(3), \qquad \mathcal{T}_c = \pm 0.08(2), \tag{39}$$

TABLE II. Parameters defined in Eq. (35), where the uncertainties come from the model calculation.

ℓ	$\mathcal{Y}_R$	$\mathcal{Y}_R'$	$\mathcal{Y}_S$	$\mathcal{Y}_P$
e	−0.238(11)	0.703(13)	$< 10^{-4}$	$< 10^{-4}$
μ	−0.237(12)	0.701(13)	−0.0037(2)	0.0136(2)
τ	−0.149(6)	0.438(8)	−0.039(2)	0.180(2)

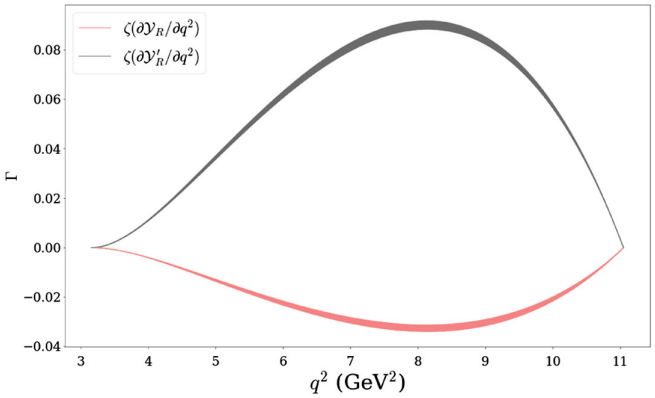

FIG. 2. q^2 dependence of $\zeta(\partial\mathcal{Y}_R^{(\prime)}/\partial q^2)$ in $\Lambda_b \to \Lambda_c\tau^-\bar{\nu}$, where the bands represent the uncertainties caused by the form factors.

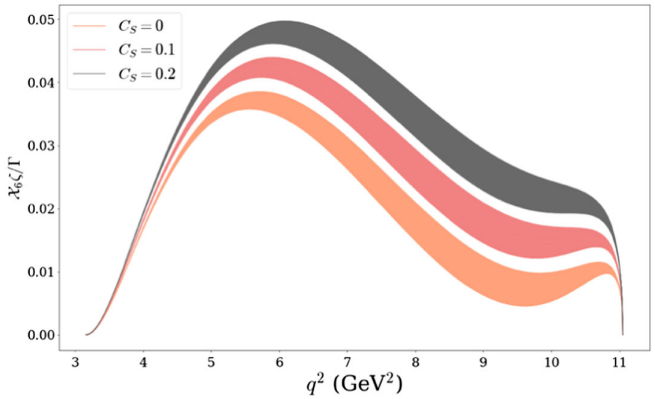

FIG. 3. q^2 dependence of $\mathcal{X}_6\zeta/\Gamma$ with $\ell = \tau$ for $C_S = 0$, 0.1 and 0.2, respectively.

for $\Lambda_b \to \Lambda_c\tau^-\bar{\nu}$. Notice that the signs are irrelevant for searching evidence of NP as long as they are nonzero. To estimate the results at LHCb run 2, we take $N_{\Lambda_b} = 5 \times 10^9$, $P_b = 0.03$, $\varepsilon = 10^{-4}$, and

$$\sum_f |\mathcal{B}(\Lambda_c \to B_n f)\alpha(\Lambda_c \to B_n f)| = 6 \times 10^{-2}, \tag{40}$$

resulting in that $|\Delta N_\ell| \approx 50$ and $\Delta N_c \approx 20$ for $\ell = \tau$, which are large and ready to be measured. Here, Eq. (40) is derived by crunching up the numbers in Eqs. (27) and (28).

To probe the effects of the scalar operators, we find that $\mathcal{X}_6$, which can be understood as a combination of A_{FB} and A_{UD}, is sensitive to $C_{S,P}$ for $\ell = \tau$. The results are plotted in Fig. 3, where we have taken $C_P = C_S$.[1] In the region of 9 GeV^2 $< q^2 <$ 10 GeV^2, $\mathcal{X}_6$ can be enhanced largely. In particular, it is twice larger with $C_S = 0.2$ in comparison to that in the SM.

[1]The scenario of $C_P = -C_S$ is ruled out by the lifetime of B_c^- [20].

V. SUMMARY

Based on the helicity formalism, we have given the full angular distributions of $\Lambda_b \to \Lambda_c(\to B_n f)\ell^-\bar{\nu}$. In particular, we have identified TR violating terms, which vanish in the SM due to the lack of relative complex phases. Since strong phases are not required in these TR violating observables in contrast to the direct CP asymmetries, they can be reliably calculated. The angular distributions have been given explicitly with the helicity amplitudes in Table I. We have cross-checked our results with those in Refs. [10,14], and found that they are consistent. Note that our results can be easily applied to $\Xi_b \to \Xi_c(\to B_n f)\ell^-\bar{\nu}$ with trivial modifications.

Notably, the effects of NP can be absorbed by redefining the helicity amplitudes as demonstrated in Eq. (31) with $\xi_\pm$ calculated in the SM. We recommend the experiments to measure the TR violating observables of $\mathcal{T}_{\ell,c}$ defined in Eq. (29) for searching NP as they vanish in the SM. To compare with the experiments, $\Delta N_{\ell,c}$ have been defined by the numbers of the observed events, which are proportional to $\mathcal{T}_{\ell,c}$. Based on $C_R = \pm 0.42(7)i$ for $\ell = \tau$, we have obtained that $|\Delta N_{\ell,c}| \approx 50$, 20 at LHCb run 2, which are sufficient for measurements. On the other hand, we have pointed out that $\mathcal{X}_6$ is sensitive to $C_{S,P}$ for $\Lambda_b \to \Lambda_c\tau^-\bar{\nu}$, which can be largely enhanced in the high q^2 region.

ACKNOWLEDGMENTS

We would like to thank Jiabao Zhang for valuable discussions. This work is supported in part by the National Key Research and Development Program of China under Grant No. 2020YFC2201501 and the National Natural Science Foundation of China (NSFC) under Grant No. 12147103.

APPENDIX A: DIRAC SPINORS

In this work, we choose fermions and antifermions in $p\hat{z}$ and $-p\hat{z}$ directions, respectively. We have that

$$u_+ = \begin{pmatrix} E_+ \\ 0 \\ E_- \\ 0 \end{pmatrix}, \quad u_- = \begin{pmatrix} 0 \\ E_+ \\ 0 \\ -E_- \end{pmatrix},$$
$$v_+ = \begin{pmatrix} E_- \\ 0 \\ -E_+ \\ 0 \end{pmatrix}, \quad v_- = \begin{pmatrix} 0 \\ -E_- \\ 0 \\ -E_+ \end{pmatrix}, \tag{A1}$$

with "±" denoting the helicities, $E_\pm = \sqrt{E \pm m}$, and m the particle mass. Notice that the relative signs are crucial, fixed by the relations

$$u_- = L_z^u R_y(\pi)(L_z^u)^{-1}u_+, \quad v_- = (L_z^v)^{-1}R_y(\pi)L_z^v v_+, \tag{A2}$$

where R_y is the rotation matrix toward $\hat{y}$, and $L_z^{u,v}$ are the Lorentz boost operators toward $\hat{z}$. Here, $L_z^{u,v}$ are taken in a way such that $L_z^{u-1}u_\pm$ and $L_z^v v_\pm$ are at rest.

APPENDIX B: ANGULAR DISTRIBUTIONS IN THE STANDARD MODEL

We now sketch the derivation of Eq. (13). We start with a two-body decay of $i \to f_1 f_2$, where i and $f_{1,2}$ are unspecific particles. The decay distribution is given as

$$\frac{\partial^2\Gamma(i \to f_1 f_2)}{\partial\phi\partial\cos\theta} \propto \sum_{\lambda_1,\lambda_2} |\langle p,\theta,\phi,\lambda_1,\lambda_2|U(\infty,-\infty)|i;J,J_z\rangle|^2, \tag{B1}$$

$$|p,\theta,\phi,\lambda_1,\lambda_2\rangle = R_z(\phi)R_y(\theta)(|f_1;\vec{p}=p\vec{z},\lambda_1\rangle \otimes |f_2;\vec{p}=-p\vec{z},\lambda_2\rangle), \tag{B2}$$

where U is the time evolution operator, J and J_z are the angular momentum and its z component of the initial particle, $R_{y,z}$ are the rotational operators pointing toward (y,z), and $\lambda_{1,2}$ are the helicities of $f_{1,2}$. In the decay distributions, we have to sum over the helicities of the outgoing particles as they are difficult to be probed in the experiments.

In two-body systems, states with definite angular momenta and helicities can be constructed as

$$|\lambda_1,\lambda_2,J,J_z\rangle = \frac{1}{(2J+1)\pi}\int d\cos\theta d\phi |p,\theta,\phi,\lambda_1,\lambda_2\rangle \times e^{iJ_z\phi}d^J(\theta)^{J_z}{}_{\lambda_1-\lambda_2}, \tag{B3}$$

along with the identity

$$1 = \sum_{J,J_z}\frac{4\pi}{2J+1}|J,J_z,\lambda_1,\lambda_2\rangle\langle J,J_z,\lambda_1,\lambda_2|. \tag{B4}$$

Notice that in Eq. (B3), $\lambda_{1,2}$ are unaltered because they are rotational scalars. By inserting Eq. (B4) in Eq. (B1), we obtain

$$\frac{\partial^2\Gamma(i \to f_1 f_2)}{\partial\phi\partial\cos\theta} \propto \sum_{\lambda_1,\lambda_2}|e^{iJ_z\phi}d^J(\theta)^{J_z}{}_{\lambda_1-\lambda_2}H_{\lambda_1\lambda_2}|^2, \tag{B5}$$

with

$$H_{\lambda_1,\lambda_2} \equiv \langle J,J_z,\lambda_1,\lambda_2|U(\infty,-\infty)|i;J,J_z\rangle. \tag{B6}$$

Clearly, H_{λ_1,λ_2} is independent of J_z since U must be a scalar. In Eq. (B5), we see that the decay distributions are separated into two different parts. The kinematic part is described by the Wigner-d matrix whereas the dynamical part by H_{λ_1,λ_2}.

The three-body decay distributions can be obtained by decomposing the systems into a product of two-body decays as demonstrated in Eq. (6).

APPENDIX C: CONTRIBUTIONS FROM SCALAR AND CURRENT OPERATORS

The contributions of C_L are given by

$$\xi_\pm \to (1+C_L)\xi_\pm, \tag{C1}$$

due to the same coupling in the SM. Furthermore, those of C_R can be obtained straightforwardly by

$$\xi_\pm \to \xi_\pm + C_R\xi_\mp, \tag{C2}$$

as $\bar{c}\gamma^\mu P_{L,R}b$ are related by the parity.

The scalar operators contribute to the amplitudes as

$$\frac{G_f}{\sqrt{2}}V_{cb}L_t^N B_t^N, \qquad L_t^N = \mathcal{C}\bar{u}_\ell P_L v_\nu,$$
$$B_t^N = \mathcal{C}^{-1}\bar{u}_c(C_S f_s + C_P g_p\gamma_5)u_b, \tag{C3}$$

where $\mathcal{C}$ is a constant, Clearly, B_t^N and L_t^N can be viewed as the transitions of $\Lambda_b \to \Lambda_c P^-$ and $P^- \to l^-\bar{\nu}$, respectively, with P^- an effective particle from NP. As P^- is spinless, $L_t^N B_t^N$ is only related to $L_t B_t$ in Eq. (6). By adjusting $\mathcal{C}$ such that $L_t^N = L_t$, we arrive at

$$t_\pm^N = t_\pm - \frac{\sqrt{Q_+ q^2}}{m_\ell}C_S f_s \pm \frac{\sqrt{Q_- q^2}}{m_\ell}C_P g_p. \tag{C4}$$

By collecting Eqs. (C1), (C2), and (C4), we obtain Eq. (31). It is interesting to see that all the contributions can be encapsulated in $\xi_\pm$, which already exist in the SM.

APPENDIX D: CONTRIBUTIONS FROM TENSOR OPERATOR

To cooperate the tensor operator with the helicity amplitudes, by utilizing Eq. (2) we decompose the products of the Minkowski metric as

$$(g^{\mu\nu}g^{\mu'\nu'} - g^{\mu'\nu}g^{\mu\nu'}) = \sum_\lambda(-V_1^{\mu\mu'}(\lambda)V_1^{\nu\nu'*}(\lambda) + V_2^{\mu\mu'}(\lambda)V_2^{\nu\nu'*}(\lambda)), \tag{D1}$$

with

$$V_1^{\mu\mu'}(\lambda) = \left(\varepsilon_t^{\mu}\varepsilon_\lambda^{\mu'} - \varepsilon_t^{\mu'}\varepsilon_\lambda^{\mu}\right),$$
$$V_2^{\mu\mu'}(\lambda) = \frac{1}{\sqrt{2}}\left(\varepsilon_{\lambda_1}^{\mu}\varepsilon_{\lambda_2}^{\mu'} - \varepsilon_{\lambda_1}^{\mu'}\varepsilon_{\lambda_2}^{\mu}\right), \tag{D2}$$

and

$$(\lambda_1,\lambda_2) = (1,0),(1,-1),(0,-1), \quad \text{for } \lambda = 1,0,-1. \tag{D3}$$

To see that $V_{1,2}$ can be viewed as spacelike vectors, in the $\vec{q}$ frame, we define

$$(\vec{V}_1)_i = V_1^{0i}, \qquad (\vec{V}_2)_i = \epsilon_{ijk}\vec{V}_2^{jk}, \tag{D4}$$

with $i,j,k = x,\ y,\ z$ and ϵ_{ijk} the totally antisymmetric tensor. It shows that V_1 and V_2 are spacelike, which are essentially spin-1 under the $SO(3)$ rotational group.

The results can be understood in terms of the group theory, given as[2]

$$(\mathbf{1}\oplus\mathbf{3})_1 \otimes (\mathbf{1}\oplus\mathbf{3})_2 = (\mathbf{1}\oplus\mathbf{3}\oplus\mathbf{6})_S + (\mathbf{3}\oplus\bar{\mathbf{3}})_A, \tag{D5}$$

where **1**, **3**, and **6** are the representations of the $SO(3)$ rotational group, and we have used the fact that a four-vector is $\mathbf{1}\oplus\mathbf{3}$. In Eq. (D5), "$S$" and "$A$" in the subscripts indicate symmetric and antisymmetric between the first and second objects, respectively. The antisymmetric nature of $\sigma_{\mu\nu}$ forces us to select the second solution, where **3** and $\bar{\mathbf{3}}$ correspond to V_1 and V_2, respectively.

Now, we are able to rewrite the transition matrix element of the tensor operator as

$$g^{\mu\nu}g^{\mu'\nu'}(\bar{u}_\ell\sigma_{\mu\mu'}P_L v)\langle\Lambda_c|\bar{c}\sigma_{\nu\nu'}b|\Lambda_b\rangle = \sum_{\lambda,n} L_\lambda^{V_n} B_\lambda^{V_n},$$
$$L_\lambda^{V_n} = \frac{(-1)^n}{2} i V_n^{\mu\mu'}(\lambda)\bar{u}_\ell\sigma_{\mu\mu'}P_L v,$$
$$B_\lambda^{V_n} = -iV_n^{\nu\nu'*}(\lambda)\langle\Lambda_c|\bar{c}\sigma_{\nu\nu'}b|\Lambda_b\rangle, \tag{D6}$$

which can be understood as a product of $\Lambda_b \to \Lambda_c V_n$ and $V_n \to \ell^-\bar{\nu}$, with V_n effectively spin-1 particles. The helicity amplitudes of the lepton sector are given as

$$(h_+^{V_1}, h_-^{V_1}) = \left(-\frac{1}{\sqrt{2}}h_-, -\sqrt{2}h_+\right),$$
$$(h_+^{V_2}, h_-^{V_2}) = \left(\frac{1}{2}h_-, h_+\right), \tag{D7}$$

with

$$h_\pm^{V_{1,2}} = L^{V_{1,2}}_{\pm\frac{1}{2}-\frac{1}{2}}\left(\lambda_\ell = \pm\frac{1}{2}, \vec{p}_\ell = -\vec{p}_\nu = p\hat{z}\right), \tag{D8}$$

describing $(V_1 \to \ell^-\bar{\nu})$ and $(V_2 \to \ell^-\bar{\nu})$, respectively. For the baryon sector, the helicity amplitudes read as

$$H^{V_n}_{\lambda_c,\lambda} = B_\lambda^{V_n}(\lambda_b = \lambda_c - \lambda, \vec{p}_c = -\vec{q} = |\vec{p}_c|\hat{z}), \tag{D9}$$

with $H^{V_n}_{\lambda_c,t} = 0$ and $V_{1,2}$ being spacelike.

The sixfold angular distributions now take the form

$$\mathcal{B}(\Lambda_c \to B_n f)\zeta(q^2)\sum_{\lambda_\ell,\lambda,\lambda_b}\rho_{\lambda_b,\lambda_b}\Bigg|A_\lambda^c\sum_{\lambda_c,\lambda_W}\Bigg[C_T h_{\lambda_\ell}^{V_1}\left(H^{V_1}_{\lambda_c,\lambda_W} - \frac{1}{\sqrt{2}}H^{V_2}_{\lambda_c,\lambda_W}\right)$$
$$+(-1)^{J_W}H_{\lambda_c,\lambda_W}h_{\lambda_\ell}\Bigg]d^{\frac{1}{2}}(\theta_b)^{\lambda_b}{}_{\lambda_c-\lambda_W}d^{\frac{1}{2}}(\theta_c)^{\lambda_c}{}_{\lambda}d^{J_W}(\theta_\ell)^{\lambda_W}{}_{\lambda_\ell-\frac{1}{2}}e^{i(\lambda_c\phi_c+\lambda_\ell\phi_\ell)}\Bigg|^2, \tag{D10}$$

which cannot be reduced to Eq. (13) by redefining the amplitudes. Thus, Table I would no longer be suitable after the tensor operator is considered.

[2] In the $SO(3)$ group, $\bar{\mathbf{3}}$ and **3** are equivalent. However, they behave differently under the $O(3)$ group, where $\bar{\mathbf{3}}$ and **3** are parity even and odd, respectively.

[1] M. Jung and D. M. Straub, J. High Energy Phys. 01 (2019) 009; Q. Y. Hu, X. Q. Li, X. L. Mu, Y. D. Yang, and D. H. Zheng, J. High Energy Phys. 06 (2021) 075; Z. R. Huang, E. Kou, C. D. Lü, and R. Y. Tang, Phys. Rev. D **105**, 013010 (2022); K. Ezzat, G. Faisel, and S. Khalil, arXiv:2204.10922; A. Datta, H. Liu, and D. Marfatia, arXiv:2204.01818; R. Y. Tang, Z. R. Huang, C. D. Lü, and R. Zhu, arXiv:2204.04357.

[2] R. Aaij *et al.* (LHCb Collaboration), Phys. Rev. Lett. **115**, 111803 (2015); **115**, 159901(E) (2015); S. Hirose *et al.*

(Belle Collaboration), Phys. Rev. Lett. **118**, 211801 (2017); R. Aaij *et al.* (LHCb Collaboration), Phys. Rev. Lett. **120**, 171802 (2018).
[3] R. L. Workman *et al.* (Particle Data Group), Prog. Theor. Exp. Phys. **2022**, 083C01 (2022).
[4] Y. S. Amhis *et al.* (HFLAV Collaboration), Eur. Phys. J. C **81**, 226 (2021).
[5] S. Jaiswal, S. Nandi, and S. K. Patra, J. High Energy Phys. 12 (2017) 060.
[6] S. Bifani, S. Descotes-Genon, A. Romero Vidal, and M. H. Schune, J. Phys. G **46**, 023001 (2019).
[7] R. Aaij *et al.* (LHCb Collaboration), Phys. Rev. Lett. **128**, 191803 (2022).
[8] F. U. Bernlochner, Z. Ligeti, D. J. Robinson, and W. L. Sutcliffe, Phys. Rev. Lett. **121**, 202001 (2018); Phys. Rev. D **99**, 055008 (2019).
[9] S. Shivashankara, W. Wu, and A. Datta, Phys. Rev. D **91**, 115003 (2015); R. Dutta, Phys. Rev. D **93**, 054003 (2016); X. Q. Li, Y. D. Yang, and X. Zhang, J. High Energy Phys. 02 (2017) 068; A. Datta, S. Kamali, S. Meinel, and A. Rashed, J. High Energy Phys. 08 (2017) 131; E. Di Salvo, F. Fontanelli, and Z. J. Ajaltouni, Int. J. Mod. Phys. A **33**, 1850169 (2018); X. L. Mu, Y. Li, Z. T. Zou, and B. Zhu, Phys. Rev. D **100**, 113004 (2019); P. Böer, A. Kokulu, J. N. Toelstede, and D. van Dyk, J. High Energy Phys. 12 (2019) 082; X. L. Mu, Y. Li, Z. T. Zou, and B. Zhu, Phys. Rev. D **100**, 113004 (2019); N. Penalva, E. Hernández, and J. Nieves, Phys. Rev. D **100**, 113007 (2019); P. Colangelo, F. De Fazio, and F. Loparco, J. High Energy Phys. 11 (2020) 032; N. Penalva, E. Hernández, and J. Nieves, J. High Energy Phys. 06 (2021) 118; N. Penalva, E. Hernández, and J. Nieves, Phys. Rev. D **101**, 113004 (2020).
[10] A. Kadeer, J. G. Korner, and U. Moosbrugger, Eur. Phys. J. C **59**, 27 (2009); T. Gutsche, M. A. Ivanov, J. G. Körner, V. E. Lyubovitskij, P. Santorelli, and N. Habyl, Phys. Rev. D **91**, 074001 (2015).
[11] Q. Y. Hu, X. Q. Li, Y. D. Yang, and D. H. Zheng, J. High Energy Phys. 02 (2021) 183; N. Penalva, E. Hernández, and J. Nieves, J. High Energy Phys. 04 (2022) 026.
[12] R. Aaij *et al.* (LHCb Collaboration), J. High Energy Phys. 06 (2020) 110.
[13] M. Ferrillo, A. Mathad, P. Owen, and N. Serra, J. High Energy Phys. 12 (2019) 148.
[14] S. Groote, J. G. Körner, and B. Melić, Eur. Phys. J. C **79**, 948 (2019).
[15] J. Y. Cen, C. Q. Geng, C. W. Liu, and T. H. Tsai, Eur. Phys. J. C **79**, 946 (2019).
[16] C. Q. Geng, C. W. Liu, and T. H. Tsai, Phys. Rev. D **103**, 054018 (2021).
[17] C. Q. Geng and C. W. Liu, J. High Energy Phys. 11 (2021) 104.
[18] S. Iguro and R. Watanabe, J. High Energy Phys. 08 (2020) 006; S. Iguro, M. Takeuchi, and R. Watanabe, Eur. Phys. J. C **81**, 406 (2021).
[19] C. W. Liu and C. Q. Geng, arXiv:2205.08158.
[20] R. Alonso, B. Grinstein, and J. Martin Camalich, Phys. Rev. Lett. **118**, 081802 (2017).